FORWARD SIMULATIONS OF PASSIVE MICROWAVE OBSERVATIONS FOR THE SOIL MOISTURE ACTIVE PASSIVE (SMAP) MISSION

Steven Chan, Eni Njoku, and Scott Dunbar

Jet Propulsion Laboratory
California Institute of Technology
Pasadena, CA 91109, USA.

ABSTRACT

In this paper, we describe our approach to simulate realistic L-band brightness temperatures to be measured by the Soil Moisture Active Passive (SMAP) mission. These realistic simulated measurements are crucial because they provide a quantitative basis by which we develop and improve our pre-launch retrieval algorithms for soil moisture at 9-km and 36-km spatial scales.

Index Terms— SMAP, soil moisture, freeze-thaw, L-band, synergy

1. INTRODUCTION

SMAP was one of the four first-tier missions recommended by the National Research Council's Committee on Earth Science and Applications from Space [1]. Scheduled for launch in late 2014, the mission will use a radiometer and a high-resolution imaging radar (both at L-band frequencies) to obtain frequent and accurate global measurements of soil moisture and freeze-thaw state over land. The resulting hydrological information will advance our understanding of the physical processes linking the water, energy, and carbon cycles, leading to improved forecasts of weather, flood, drought, and agricultural productivity.

To prepare for the science return of the mission, the SMAP team is currently developing a suite of retrieval algorithms and testing them against various validating data sources, including (a) existing satellite data records, (b) field campaign matchup data, and (c) simulated observations.

In this paper, we have our focus on (c) and describe our approach to generate simulated SMAP passive (radiometer) observations for coarse-scale soil moisture retrieval. The approach to simulate the SMAP active (radar) observations for fine-scale retrieval of soil moisture and freeze-thaw is similar and is not emphasized here.

2. GLOBAL SIMULATION

For the purpose of testing and developing pre-launch SMAP retrieval algorithms, it is necessary to be able to simulate the native radar and radiometer observations as realistically as possible. Furthermore, the simulation domain should be global in extent so that the performance of the algorithms can be gauged under as wide a range of geophysical conditions as possible.

To achieve these goals, we had identified and implemented the major simulation modules needed to describe the end-to-end data acquisition process of SMAP. There are five major modules and they are: (a) land surface model (LSM) output, (b) spacecraft orbital and instrument sampling, (c) land forward model, (d) instrument and environmental uncertainty, and (e) Earth-fixed gridding. The simulation flow among these modules is described in Fig. 1.

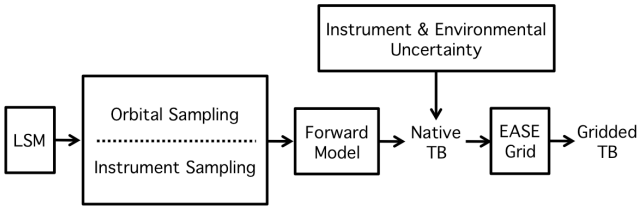

Figure 1: The five major modules for realistic simulation of SMAP brightness temperature (TB) measurements. LSM outputs, along with some static geophysical parameters (e.g. sand fraction), are first sampled in a way consistent with the SMAP's orbit and scanning geometry. The sampled outputs then go through the land forward model to generate the time-ordered H- and V-polarized TB's at 1.4 GHz. The native TB's are then perturbed with instrument and environmental uncertainty before being remapped on an EASE Grid [2]. The resulting gridded TB's are then used for soil moisture retrieval at 36 km.

2.1. Land surface model output

To initialize our forward simulation, we begin with an LSM that is driven and constrained by dynamic meteorological and geophysical forcings. For any particular snapshot in time, the model produces synoptic estimates of soil moisture and soil temperature over the geographical domain of interest.

The LSM output that we used for forward simulation is merged from two LSM sources. The first LSM source covers the North America domain at a fine spatial resolution (0.01-deg); the other LSM source (GLDAS [3]) covers the global domain at a coarse spatial resolution (0.25-deg). These LSM sources are based on the Noah LSM and are available every 6 hours for the entire year of 2003 for our simulation.

Logistically, the merging of both fine- and coarse-scale LSM output parameters is intentional: by it we will be able to use just one integrated input dataset to test and develop the entire suite of SMAP retrieval algorithms, including the active, passive, and the combined active and passive algorithms. In addition, the global extent of the simulation provides a realistic coding context for our codes to conform

to the software specification of the future SMAP operational software.

2.2. Spacecraft orbital and instrument sampling

SMAP was designed to acquire data in a sun-synchronous 8-day exact repeat orbit, with a local time descending node (LTDN) at 6:00 am. The resulting orbit pattern repeats itself every 8 days and provides global data acquisition in 2-3 days.

To simulate this space-time sampling pattern of SMAP TB's as realistically as possible, we developed codes to generate an enormous ephemeris database for the time stamps and instantaneous positions (boresight locations and groundtrack locations) of the spacecraft for one full year. Along with ephemeris data, this database also describes the antenna gain information and ground locations within the half-power beamwidth (HPBW) of the SMAP's conically scanning antenna. For easier data management, the database was split into two sections. The ascending (6:00 am) half-orbit section began from the southernmost latitude; the descending (6:00 pm) half-orbit section began from the northernmost latitude.

The entire database was then used along with a land forward model (Section 2.3) to generate the simulated TB's.

2.3 Land forward model

Given the time stamps and instantaneous positions of the spacecraft described in the previous section, we sampled the underlying LSM static and dynamic data fields at the same time stamps and positions described in the database. The resulting sampled fields then went through a land forward model to compute a 'mesh' of simulated TB's within the HPBW. To synthesize the simulated antenna temperature received by the antenna, we integrated the simulated TB's based on the SMAP's antenna pattern over the solid angle subtended by the HPBW.

By having LSM data fields sampled within the HPBW, we are able to explicitly account for sub-footprint surface heterogeneity arising from (a) nonlinear spatial aggregation of finer-scale geophysical parameters (e.g., soil texture and vegetation water content) and (b) mixed pixels due to land and open static or transient water.

Over land locations, we used the *tau-omega* model to convert the sampled LSM fields into simulated TB observations. Model coefficients (e.g., surface roughness, single scattering albedo) that tend to vary with land cover types were applied through a table-lookup approach similar to those described in [4-5]. Over water locations, we used the Klein-Swift model [6], assuming, for the sake of simplicity, zero salinity and constant water temperature of 20 deg C everywhere. Wherever there was a mix of land and water within the HPBW, their relative TB contributions were determined from their relative area fractions in the footprint. The result was a 'clean' (i.e., noise-free) version of the simulated H-polarized and V-polarized TB's at 1.4 GHz.

To date, however, we had not developed reliable radiative transfer models to simulate TB emission from snow or permanent ice sheets.

2.4 Instrument and environmental uncertainty

As mentioned earlier, the simulated TB's resulting from the above modeling process were 'clean' – they did not account for the impacts of error sources on TB measurement. In reality, these error sources are of diverse nature and some of them are significant drivers behind the total radiometer error budget. These error sources typically fall into two categories: (a) instrument uncertainty, which refers to the total combined impacts of thermal noise, calibration bias, sidelobe TB contribution, and cross-polarization leakage, and (b) environmental uncertainty, which refers to the total uncorrected TB contribution due to Faraday rotation, solar radiation (direct and reflected), galactic radiation, cosmic background radiation, and atmospheric absorption. To properly account for these error sources, their unique variability characteristics must be observed: some error terms may be adequately modeled as simply as random variables; others need to be considered as fixed or slowly-varying biases that vary with latitudes and longitudes and/or season of the year.

For our simulation purposes, given the SMAP's designed accuracy of 1.3K for TB measurements over a 30 km × 30 km grid cell, it is necessary to maintain the fixed part of this 1.3K error while scaling up the random part of it according to $\sqrt{N}$, where N is the number of natively sampled TB's (both fore- and aft-looks) falling into the 30 km × 30 km grid cell. Based on our current best estimates, the random error associated with individual time-ordered TB's was about 2.6K.

2.5 Earth-fixed gridding

Our forward simulations concluded with binning the time-ordered TB's on an Earth-fixed grid. This process prepared the resulting gridded TB's for subsequent geophysical inversion, which involved ancillary data sources that were also defined on certain Earth-fixed grids. Both fore- and aft-looks of TB's from a given orbit granule (ascending pass or descending pass) were combined to produce the TB at a given grid cell.

At present, a modified version of the original global 25-km EASE Grid [2] was selected for the SMAP radiometer-derived soil moisture data product. This modified version has a nominal grid resolution of 36 km, which was chosen to match the dimension of the SMAP's radiometer footprint. The resulting grid has 408 rows and 963 columns, covering [86.62°S, 86.62°N] in latitudes and [180.00°W, 180.00°E] in longitudes. The area of each grid cell is exactly 36 km × 36 km, or 1,296 km^2.

Like the original EASE Grid, this 36-km EASE Grid is also scalable – the same grid transformation procedures can be applied to construct a family of EASE Grids of various grid resolutions. With proper grid parameters, an EASE Grid of finer-scale grid resolution can be made to completely "nest" within an EASE Grid of coarser-scale grid resolution. The resulting multi-scale grid system, in the context of SMAP Level 2 and 3 data products, provides a natural way to simultaneously accommodate the coarse-scale passive soil moisture products, the fine-scale active soil moisture and freeze-thaw products, as well as the intermediate-scale active-passive soil moisture products.

Besides the above benefits, EASE Grid has a long heritage in satellite passive microwave data records beginning from SMMR, SSM/I, to AMSR-E. SMAP's adoption of the EASE Grid will make its data products a

potential valuable collection that helps extend the existing radiometer-based hydrological data records.

3. RESULTS

Following the above steps, a full year of simulated gridded TB's was generated to enable evaluation of retrieval algorithms subject to the natural dynamic range and spatial correlation of geophysical conditions. In our forward simulations, permanent ice sheets were approximated as frozen bare soils whose dielectric constant was modeled using the approach described in [7]. Because our LSM data sources did not extend beyond 60°S, no simulated TB's were generated over the Antarctic.

Figure 2 shows a "snapshot" of the gridded simulated H-polarized TB acquired between Jun 1–3, 2003 from a total of 44 descending (6:00 am) half orbits. The simulated TB displays a spatial variability that is consistent with major land cover types (e.g., arid regions, densely vegetated areas). Furthermore, it confirms that the SMAP's 8-day exact repeat orbit provides complete global coverage within 3 days.

Figure 3 shows the one-year (2003) time series of the gridded simulated H-polarized TB from a total of 136 descending (6:00 am) half orbits. The series were extracted at two locations of contrasting land cover types. The upper panel corresponds to an arid location (24.42°N, 21.68°E) within the Sahara desert, where the land emission is predominantly governed by the highly dynamic surface temperature. This is correctly reflected by the simulated TB time series, which exhibits a large annual cycle in variability that reaches a maximum over the Jun–Jul-Aug (JJA) season. Overall, the time series has a standard deviation of 10.3K.

The lower panel in the figure corresponds to a densely vegetated location (2.95°S, 62.43°W) within the Amazon forest. The large opacity at microwave frequencies of this location makes it a good approximation to an ideal and stable blackbody emitter. Accordingly, microwave emission from this location is expected to remain stable, as supported by the simulated TB time series that vary as little as 3.9K (standard deviation) throughout the year.

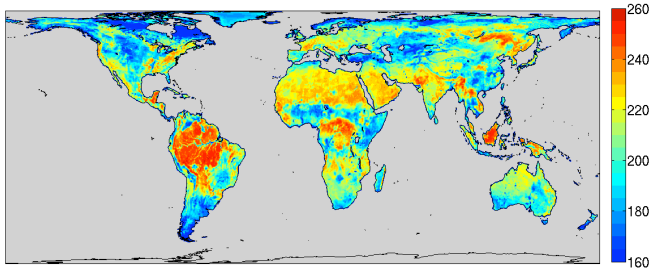

Figure 2: Global simulated L-band H-polarized TB between Jun 1–3, 2003. The data were generated using an analytical approach consistent with the actual physical emission process. Ocean TB's, though simulated, were not displayed in order to maximize the limited data range for displaying TB variability over land.

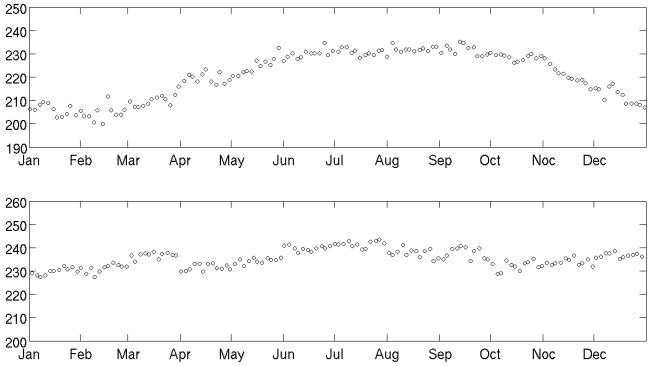

Figure 3: Time series of simulated H-polarized TB at an arid location (upper panel) and at a densely vegetated location (lower panel). In terms of variability (or lack of it), the results are consistent with the land forward model used in the simulation. Given the SMAP's 8-day exact repeat orbit, there are 136 TB observations at either location, resulting in an average revisit frequency of 365/136, or 2.7 days at the latitudes of these locations.

4. SUMMARY

In this paper, we describe our attempt to perform realistic simulations of SMAP brightness temperatures soil moisture retrieval at 36-km spatial scales. The procedure takes into account such factors as orbital sampling, instrument sampling, instrument and environmental uncertainty, and data remapping on an Earth-fixed grid. An annual cycle of simulated H- and V-polarized TB's had been generated as a baseline testing dataset on which the performance of retrieval algorithms is to be evaluated. The gridded simulated TB time series shows consistent variations over arid and densely vegetated areas.

5. ACKNOWLEDGEMENTS

The work described in this paper was performed by the Jet Propulsion Laboratory, California Institute of Technology, under a contract with the National Aeronautics and Space Administration.

6. REFERENCES

[1] The National Research Council, *Earth Science and Applications from Space: National Imperatives for the Next Decade and Beyond*, National Academy Press, Washington, D.C., 2007.

[2] The National Snow and Ice Data Center (NSIDC), "EASE-Grid Data." [Online] Available: http://nsidc.org/data/ease/. [Accessed: Dec 10, 2009].

[3] Goddard Space Flight Center (GSFC), "LDAS: Land Data Assimilation Systems." [Online] Available: http://ldas.gsfc.nasa.gov/gldas/ [Accessed: Jun 29, 2010].

[4] Crow, W., T. Chan, D. Entekhabi, P. Houser, T. Jackson, E. Njoku, P. O'Neill, J. Shi, and X. Zhan, "An observing system simulation experiment for SMAP radiometer soil

moisture products," *IEEE Trans. Geosci. Remote Sens.,* 43(6), pp. 1289–1303, 2005.

[5] Crosson, W. L., A. Limaye, and C. Laymon, "Impacts of Spatial Scaling Errors on Soil Moisture Retrieval Accuracy at L-Band." *IEEE Journal of Selected Topics in Applied Earth Observations and Remote Sensing*, (3)1, pp. 67–80, 2010.

[6] Klein, L. A. and C. T. Swift, "An improved model for the dielectric constant of seawater at microwave frequencies," *IEEE Trans. Ant. Propagat.*, AP-25, No. 1, pp. 104–111.

[7] Zhang, L., J. Shi, Z. Zhang, K. Zhao, "The estimation of dielectric constant of frozen soil-water mixture at microwave bands," *Proc. 2003 IEEE International Geoscience and Remote Sensing Symposium (IGARSS 2003)*, Toulouse, France, Jul 21–25, 2003.